CAPACITÀ ROTAZIONALE DI ELEMENTI IN ACCIAIO A SEZIONE CAVA FORMATI A FREDDO

ROTATION CAPACITY OF STEEL MEMBERS WITH COLD-FORMED HOLLOW CROSS-SECTION

Melina Bosco,
Carmelo Pannitteri
Pier Paolo Rossi
University of Catania
Department of Civil Engineering and Architecture
Catania, Italy
mbosco@dica.unict.it
carmelo.pannitteri@phd.unict.it
prossi@dica.unict.it

Mario D'Aniello
Raffaele Landolfo

University of Naples Federico II
Department of Structures for Engineering and Architecture
Naples, Italy
mdaniel@unina.it
landolfo@unina.it

ABSTRACT

Cold formed Hollow Structural Sections (HSS) are widely used in structural applications because of their high strength-to-weight ratio and torsional stiffness. Current European seismic code provides limited rules and guidance to evaluate the plastic rotation capacity of HSS members. Within the framework of revision of Eurocodes, still in progress, the research activity carried out in this study is aimed at developing formulations to predict the rotation capacity of cold formed HSS columns. To this end, parametric finite element simulations were carried out on a comprehensive set of members with different shape of cross sections (i.e. both square and rectangular HSS), local and global slenderness, shear length and axial load. The adopted finite element models were calibrated against results of cyclic experimental tests available from the literature. The results of the parametric analysis were processed in order to derive analytical equations predicting the rotation capacity at both significant damage and near collapse limit states.

SOMMARIO

Le sezioni scatolari in acciaio piegate a freddo sono ampiamente utilizzate in virtù dell'elevata rigidezza torsionale e dell'elevata resistenza che è possibile raggiungere utilizzando sezioni di modeste dimensioni. Tuttavia, l'attuale Eurocodice 8 fornisce indicazioni limitate riguardo alla

stima della duttilità e delle rotazioni plastiche che elementi realizzati mediante tali profilati sono capaci di sostenere.
Nell'ambito del processo di revisione degli Eurocodici, attualmente in corso, il presente lavoro è finalizzato allo sviluppo di una formulazione analitica per la stima della capacità rotazionale di colonne realizzate mediante profilati a sezione scatolare piegati a freddo. A questo scopo, sono condotte delle analisi parametriche considerando un insieme di colonne che differiscono per forma della sezione trasversale (rettangolare o quadrata), per la snellezza locale e globale, per la luce di taglio e per lo sforzo normale agente. Il modello numerico agli elementi finiti è preliminarmente validato mediante il confronto con i risultati di prove sperimentali disponibili in letteratura.
I risultati delle analisi numeriche sono utilizzati per calibrare equazioni per la stima della capacità rotazionale allo stato limite di danno severo e prevenzione del collasso.

1 INTRODUCTION

Recently, research on cold-formed box profiles (HSS) has been focused on the evaluation of the cyclic response of beams [1] and columns [2]. Further, numerical models [3-4] have been developed to identify suitable ranges of the width-to-thickness and depth-to-thickness ratios to guarantee stable hysteretic behavior up to a rotation of 0.04 rad. Despite the growing interest in HSS members, limited rules are provided in European seismic codes to estimate the rotational capacity of HSS beams and columns. In regard to the design of highly ductile and moderately ductile moment resisting frames, Eurocode 8 [5] stipulates that the selected cross-sections should be classified as Class 1 or 2 according to Eurocode 3 (EC3) [6]. Further, the rotation capacity of members with Class 1 or Class 2 cross-sections is expressed as a multiple of the chord rotation at yield and is null in columns subjected to axial force greater than 0.3 times the plastic resistance [7].
The above provisions have three main drawbacks: (1) the EC3 classification of cross-sections is based on the monotonic response of members, thus ignoring the degradation due to the cumulation of plastic deformation; (2) experimental activity on columns has shown a significant dependency of the deformation capacity on the axial force; (3) the limit values of the chord rotation capacity are given independently of the shape of the cross-section, i.e. the same limit values are given for wide flange or HSS cross-sections.
The research activity carried out in this study aims to numerically investigate the hysteretic flexural performance of cold-formed HSS members. To this end, a refined finite element model is first validated against experimental tests. Subsequently, an extensive parametric investigation is carried out on cantilever members with different width-to-thickness ratio, depth-to-thickness ratio, shear length and applied axial load. Based on the results obtained from cyclic analyses, analytical equations are proposed to predict the rotation capacity at the significant damage and near collapse limit states.

2 FINITE ELEMENT MODELS

2.1 Modelling assumptions

Finite element models are developed using ABAQUS 6.14 [8]. A cantilever structural scheme is used for all the analyzed members (Fig. 1a). To reduce the computational effort, the numerical model consists of two parts: a "fixed end part" that extends from the fixed end to twice the depth of the member from the fixed end, and a "displaced end part" that models the remaining part of the member. The link between the two parts is defined by means of a beam-type multi-point constraint. The fixed end part is modeled by 3D solid elements, while the displaced end part is modeled by means of one-dimensional elastic elements (quadratic elements of type B32 with a length of about 50 mm).

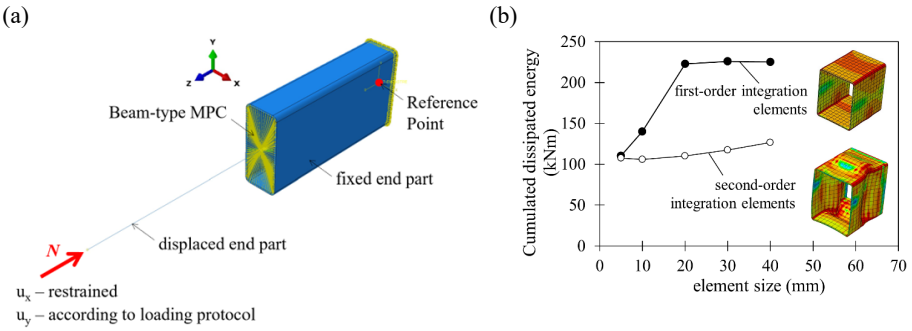

Fig. 1. (a) Numerical model; (b) Influence of the element-size on cumulated dissipated energy.

The geometry of the cross section of the fixed end part consists of four flat parts and four corner regions. Due to the process of cold forming of sections, different material properties are assigned to elements belonging to the corner and flat regions of the cross section. In any case, isotropic hardening is neglected, whereas kinematic hardening is introduced by combining the effect of N hardening components α_k (back-stress), according to Eq. (1):

$$\alpha = \sum_{k=1}^{N} \alpha_k \tag{1}$$

where $\alpha = \sigma - \sigma_0$ and σ_0 is the yield stress at zero plastic strain.
The evolution law of each kinematic component of hardening is defined as in Eq. (2):

$$\dot{\alpha}_k = C_k \frac{1}{\sigma_0}(\sigma - \alpha)\dot{\bar{\varepsilon}}^{pl} - \gamma_k \alpha_k \dot{\bar{\varepsilon}}^{pl} \tag{2}$$

where $\dot{\bar{\varepsilon}}^{pl}$ is the equivalent plastic deformation rate and C_k and γ_k are parameters to be determined.
Due to the manufacturing process of cold-formed HSS elements, significant residual stresses occur. The intensity of these stresses in the flat ($\sigma_{rb,\ flat}$) and corner ($\sigma_{rb,\ corner}$) regions of the cross section are determined according to the formulation proposed in [9].
Geometric imperfections are introduced in the fixed end part by combining the first two buckling modes. The value of the imperfection imposed is equal to 80% of the geometric tolerance of manufacture, which is equal to 0.8% of the width of the cross section [10].
To optimize the size of the finite elements, a sensitivity analysis was carried out with reference to the specimen HSS 254×203×6.4 tested in [1]. Either first-order (linear) interpolation hexahedra or second-order (quadratic) interpolation hexahedra (C3D20R elements) with different mesh size were used. Independently of the mesh size and element type, 3 elements are considered over the thickness of the plates.
The tip of the beam is subjected to the experimental displacement protocol described in [1] and the cumulative dissipated energy has been determined at the end of each loading cycle. Figure 1b shows the prediction of the dissipated energy at the end of the loading protocol varying the mesh features. The dissipated energy increases significantly with the size of the element if first-order integration elements are used because local buckling does not occur within the plastic hinge using an element size not smaller than 20 mm. Conversely, if second order interpolation elements are used, the dissipated energy is only slightly affected by the element size. Based on the above-mentioned results and computational burden, second-order (quadratic) interpolation hexahedra elements are used with an element size equal to 20 mm.

2.2 Validation of finite element models

The FE model was validated against the results of experimental cyclic tests carried out on cantilever beams [1-2] and columns [3]. Only the experimental results of the HSS sample 254×203×6.4 tested by [1] are here reported. The length L of the beam is 1537 mm. The values of the mechanical parameters used to model the material properties are summarized in Figure 2a and are based on the data provided in [2].

The tip of the beam is subjected to the experimental protocol of lateral displacement u given in [1] and the obtained cyclic response expressed in terms of bending moment vs chord rotation ($\theta=u/L$) is plotted by a black continuous line in Figure 2b. For comparison, in the same figure the experimental hysterical response is shown by a dashed red line. The accuracy in the prediction of the cyclic response was verified in terms of cumulative dissipated energy (CDE) by calculating the following percentage error:

$$\text{Err}\ (\%) = (\text{CDE}_{\text{FEM}} - \text{CDE}_{\text{exp}})/\ \text{CDE}_{\text{exp}} \quad (3)$$

where CDE_{FEM} and CDE_{exp} are the cumulative dissipated energy determined by integrating the cyclic bending moment-chord rotation response from FE analysis and experimental testing, respectively. The error is equal to 3.35%, which confirms the satisfactory accuracy of the modeling assumptions adopted.

(a) Properties of the material model

	Flat	Corner
Es [MPa]	181000	193000
σ_0 [MPa]	412.0	519.0
C_1 [MPa]	2426.3	23251.9
γ_1	17.50	814.10
C_2 [MPa]	15453.1	9769.4
γ_2	809.5	202.70
C_3 [MPa]	0.0	7.70
γ_3	--	1.4
σ_{rb} [MPa]	±262.60	±144.43

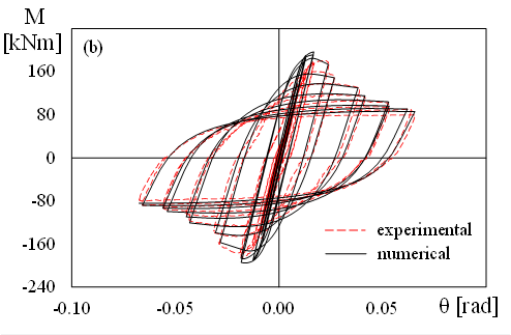

Fig. 2. Comparison between experimental and numerical cyclic responses.

3 PARAMETRIC ANALYSIS

The numerical model described in the previous section has been used to simulate the monotonic and cyclic responses of a large set of beams and columns. To this end, steel grade and cross-sections representative of square and rectangular HSS commonly used in Europe are considered.

To simulate the material properties of European profiles, some material coupon tests have been carried out at the University of Naples "Federico II" on samples extracted along the direction of rolling from the four flat parts and from the four corners of cold formed profiles with cross-section 200×200×8 and steel grade S355 JR.

The non-linear part of the stress-strain curve is given by the values of C_k and γ_k in Table 1. The values of the residual stresses are reported in the same table.

The flexural resistance and rotation capacity of steel members are strongly affected by the local slenderness of flanges and webs and thus HSS cross-sections are selected to cover b_f/t ratios ranging from 3.4 to 34, and h_w/t ratios ranging from 14 to 62.6, where b_f and h_w are the dimensions of the flat parts, i.e. are respectively equal to the width b, and the height h of the cross section reduced by two times the exterior radius of the corner.

The shear length L_V (i.e., the distance from the point of null bending moment to the fix end) is equal to the length L of the cantilever and is fixed equal to either 1.50 m, 2.25 m, 3.00 m, 3.50 m or 4.00 m so that the ratio L_V/h is in the range from 3.0 to 16.0. Finally, the axial load ratio ν ranges from 0 to 0.3.

Four classes of cross-sections are defined in EC3. The limiting values of the ratios b_f/t and h_w/t given in EC3 depend on the yield strength of steel and on the portion of the web in compression. These values are here derived assuming a yield stress f_y equal to 467.4 MPa (i.e. the yield strength of the flat parts of the FE models) and a Young's modulus equal to 200000 MP. Based on the abovementioned assumptions, 29 of the considered sections are classified as Class 1, 8 as Class 2, whereas 7 cross sections exceed limit values given for Class 2.

Table 1. Properties of the material model used in the parametric study.

Material	σ_0 [MPa]	C_1 [MPa]	γ_1	C_2 [MPa]	γ_2	σ_r [MPa]
Flat	467.4	129912	17667.9	1359.3	15.9	±306.92
Corner	402.9	180605	930.9	6.4	499.3	±168.81

4. LOADING PROTOCOLS AND MONITORED RESPONSE PARAMETERS

Cyclic analyses are carried out per examined case. The displacement applied to the tip of the cantilever along the y-direction is defined according to the loading protocol given in AISC 341-16 for the qualification of beam-to-column connections.

The cyclic response of each specimen in terms of chord rotation versus bending moment at the fixed end of the cantilever is used to evaluate (1) the first-cycle envelope curve; (2) the maximum bending moment M_{max} and the corresponding chord rotation θ_{Mmax}; (3) the chord rotation $\theta_{80\%}$ at the achievement of a residual bending moment equal to 80% of the plastic flexural resistance reduced because of the axial force $M_{pl,N}$; (4) the chord rotation $\theta_{50\%}$ at the achievement of a residual bending moment equal to 50% of $M_{pl,N}$. The chord rotations $\theta_{80\%}$ and $\theta_{50\%}$ are used to estimate the rotation capacity at significant damage (SD) and near collapse (NC) limit states, respectively. As an example, Figure 3a shows the hysteretic and first-cycle envelope curves for specimen HSS250×450×12.5 with L_V=3.5 m, whereas Figure 3b shows the monitored parameters extracted from an envelope curve.

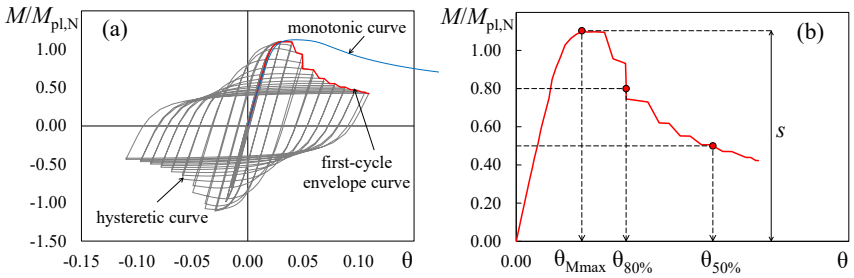

Fig. 3. Response parameters for specimen HSS250×450×12.5 with L_V=3.5 m: (a) hysteretic, monotonic and first-cycle envelope curves; (b) monitored response parameters.

5 ACCURACY OF PROVISIONS GIVEN IN EC8-PART 3

According to current Eurocode 8-part 3, cross sections of beams and columns subjected to an axial load ratio not greater than 0.3 and belonging to Class 1 should have a plastic rotation capacity not lower than 6 θ_y and 8 θ_y at SD and NC limit states, respectively. Smaller rotation capacities, equal to 2 θ_y and 3 θ_y are expected in the case of cross-sections belonging to Class 2. To comment on the accuracy of these provisions, the 16%, 50% and 84% percentiles of the rotations $\theta_{80\%}$ and $\theta_{50\%}$ exhibited by the considered members have been determined assuming that the values obtained for members with the same cross-section classification are distributed according to a lognormal distribution. The obtained values are reported in Figure 4, where the dot represents the 50% percentile and two horizontal dashes represent the 16% and 84% percentiles. The figure shows that the rotation capacity is smaller than the expected value and that the cyclic rotation capacity is significantly affected by the axial load ratio, expecially when $\theta_{50\%}/\theta_y$ is considered.

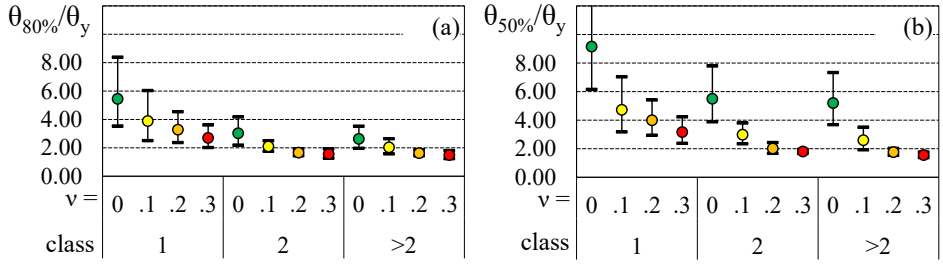

Fig. 4. Effect of the axial load ratio on the normalized cyclic chord rotation capacity: (a) SD limit state, (b) NC limit state

6 ANALYTICAL PREDICTION OF THE ROTATION CAPACITIES

Analytical equations have been derived to predict the rotation capacities $\theta_{80\%}$ and $\theta_{50\%}$ as linear combinations of multiple geometric and mechanical parameters affecting the cyclic response of HSS members. The linear combination coefficients are then determined to minimize the sum of the square of the differences between the values provided by the predictive equations and the target values obtained from the finite element simulations. More details can be found in [11].

The selected parameters for the developed predictive equations are consistent with those used in previous studies [4, 12-15]. The equations used to predict the rotation capacities $\theta_{80\%}$ and $\theta_{50\%}$ are:

$$\theta_{80\%,\text{pred}} = C_{1,80\%}\frac{1}{\lambda_f^2} + C_{2,80\%}\frac{1}{\lambda_w^2} + C_{4,80\%}\frac{L_V}{b_f} + C_{6,80\%}\frac{L_m}{L_V} + C_{7,80\%}\frac{2bt}{h\,L_V} + C_{8,80\%} \quad (4)$$

$$\theta_{50\%,\text{pred}} = C_{1,50\%}\lambda_f + C_{2,50\%}\lambda_w + C_{4,50\%}\frac{L_V}{b_f} + C_{6,50\%}\frac{L_m}{L_V} + C_{7,50\%}\frac{2bt}{h\,L_V} + C_{8,50\%} \quad (5)$$

where λ_f and λ_w are the flange and web slenderness, and L_m is the half-wave length of the buckled flange calculated as proposed in [12].

The proposed combination coefficients are reported in Table 2, whereas the comparison between the values of $\theta_{80\%}$ and $\theta_{50\%}$ predicted by the proposed equations and those provided by the numerical analyses are reported in Figure 5. In this latter figure, results referring to members characterized by axial load ratios equal to 0.0, 0.1, 0.2 and 0.3 are indicated by circles, triangles, crosses and squares, respectively. The proposed values fit well the results of the finite element simulations. Indeed, the square of the Pearson product moment correlation coefficient (R^2) is equal to 0.97 for both the rotation capacities $\theta_{80\%}$ and $\theta_{50\%}$.

Table 2. Coefficients for the proposed evaluations of the rotation capacity at SD limit state and NC limit state

	$\theta_{80\%}$	$\theta_{50\%}$
C_1	$(-10.1\,\nu^2 + 0.9) \times 10^{-3}$	$-0.274\,\nu^2 + 0.164\,\nu - 0.025$
C_2	$0.19\,\nu^2 - 0.114\,\nu + 0.025$	$0.0254\,\nu - 0.0241$
C_4	0.39×10^{-3}	$(-\nu + 0.80) \times 10^{-3}$
C_6	$0.2926\,\nu - 0.102$	$-1.48\,\nu^2 + 0.888\,\nu - 0.171$
C_7	$13.69\,\nu^2 - 8.1\,\nu + 1.2$	$43.3\,\nu^2 - 23.65\,\nu + 3.42$
C_8	$-0.0474\,\nu + 0.023$	$0.828\,\nu^2 - 0.497\,\nu + 0.117$

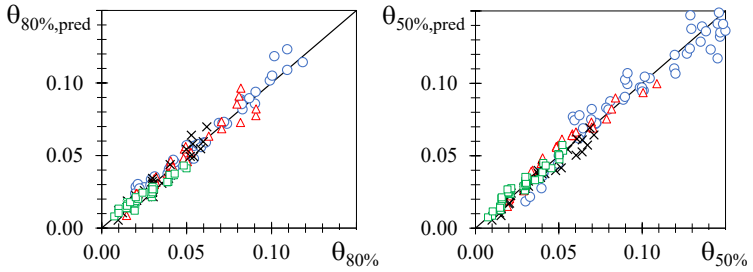

Fig. 5. Comparison between predicted and target values of the rotation capacity at SD and NC limit states

7 CONCLUSIONS

The results of numerical analyses shown in this paper highlight that the rotation capacities of members with cross-sections belonging to the same ductility class are rather scattered and are highly affected by the axial load ratios, even for their low values. In any case, rotation capacities at significant damage and near collapse limit states are significantly smaller than those given in Eurocode 8-part 3.

Starting from these considerations, equations have been proposed to predict the rotation capacity at both the SD and NC limit states. The proposed equations have the main advantage of providing rotation capacities that are not dependent on a classification of the cross-sections but vary continuously with the geometric and mechanical properties of the cross-section and structural member. Thus, the proposal overcomes the inconsistencies of current EN1998-3 for steel frames and is in line with the aims of the upcoming versions of Eurocode 8.

Finally, it should be noted that the proposed equations are applicable for structural members characterized by values of geometric and mechanical parameters within the ranges of variation considered in this study.

ACKNOWLEDGMENT

This study was partially supported by the program of University of Catania within the research project “Piano di incentivi per la ricerca di Ateneo 2020/2022 (Pia.ce.ri.) – Starting Grant” of Department of Civil Engineering and Architecture.

The experimental tests on coupon materials were funded by the Research Fund for Coal and Steel under grant agreement No. 749959 (INNO3DJOINTS);

The authors wish to thank Professor Jason McCormick and Professor Masahiro Kurata, who kindly shared the results of their experimental tests that are used in this paper to verify the effectiveness of the numerical model.

REFERENCES

[1] Fadden M., McCormick J. Cyclic quasi-static testing of hollow structural section beam members, Journal of Structural Engineering 2012; 138 (5): 561 – 570.
[2] Kurata M., Nakashima M., Suita K. Effect of column base behaviour on the seismic response of steel moment frames, Journal of Earthquake Engineering 2005; 9 (2): 415 – 438.
[3] Fadden M., McCormick J. Finite element model of the cyclic bending behavior of hollow structural sections, Journal of Constructional Steel Research 2014; 94: 64 – 75.
[4] Sediek O.A., Wu T.-Y. McCormick J., El-Tawil S. Collapse Behavior of Hollow Structural Section Columns under Combined Axial and Lateral Loading. Journal of Structural Engineering, 2020; 146(6): 0402009.
[5] CEN. EN 1998-1. EuroCode 8: Design of structures for earthquake resistance – Part 1: General rules, seismic actions and rules for buildings. Bruxelles: European Committee for Standardization; 2004.
[6] CEN. EN 1993-1-1. Eurocode 3: Design of steel structures – Part 1-1: General rules and rules for buildings. Bruxelles: European Committee for Standardization; 2006.
[7] CEN. EN 1998-3. EuroCode 8: Design of structures for earthquake resistance. Part 3: Assessment and retrofitting of buildings, Bruxelles: European Committee for Standardization; 2005.
[8] Dassault (2014), Abaqus 6.14 - Abaqus Analysis User's Manual, Dassault Systèmes Simulia Corp.
[9] Somodi B., Kövesdi B. Residual stress measurements on cold-formed HSS hollow section columns, Journal of Constructional Steel Research 2017; 128: 706 – 720.
[10] UNI EN 10219-2:2006. Cold formed welded structural hollow sections of non-alloy and fine grain steels - Part 2: Tolerances, dimensions and sectional properties, 2006.
[11] Bosco M, D'Aniello M, Landolfo R, Pannitteri C., Rossi PP. Overstrength and deformation capacity of steel members with cold-formed hollow cross-section. Journal of Constructional Steel Research 2022; 191: 107187
[12] D'Aniello M., Landolfo R., Piluso V., Rizzano G. Ultimate behavior of steel beams under non-uniform bending, Journal of Constructional Steel Research 2012; 78: 144–158.
[13] Bosco M, Tirca L. Numerical simulation of steel I-shaped beams using a fiber-based damage accumulation model. Journal of Constructional Steel Research 2017; 133: 241-255
[14] Lignos D G, Hartloper A R, Elkady A, Deierlein G G, Hamburger R, Proposed Updates to the ASCE 41 Nonlinear Modeling Parameters for Wide-Flange Steel Columns in Support of Performance-Based Seismic Engineering. Journal of Structural Engineering 2019; 145(9): 04019083
[15] Mohabeddine A, Koudri Y W, Correia J A F O, Castro J M. Rotation capacity of steel members for the seismic assessment of steel buildings. Engineering Structures 2021; 244: 112760.

KEYWORDS

Cold formed Hollow Structural Sections, rotation capacity, steel members, finite element models.